Journal of Sciences, Islamic Republic of Iran 21(1): 75-83 (2010) http://jsciences.ut.ac.ir
University of Tehran, ISSN 1016-1104

Optimization of Electrochemical Etching Parameters in FIM/STM Tungsten Nanotip Fabrication

Gh. Tahmasebipour,[1] V. Ahmadi,[2,*] and A. Abdullah[3]

[1] *Mechanical Engineering Department, Faculty of Engineering, Tarbiat Modares University, Tehran, Islamic Republic of Iran*
[2] *Electrical Engineering Department, Faculty of Engineering, Tarbiat Modares University, Tehran, Islamic Republic of Iran*
[3] *Faculty of Mechanical Engineering, Amirkabir University of Technology, Tehran, Islamic Republic of Iran*

Received: 7 January 2009 / Revised: 21 January 2010 / Accepted: 17 February 2010

Abstract

Field Ion Microscopy (FIM) and Scanning Tunneling Microscopy (STM) have found a wide application in nanotechnology. These microscopes use a metallic nanotip for image acquisition. Resolution of FIM and STM images depends largely on the radius of nanotip apex; the smaller the radius the higher the resolution. In this research, for tungsten nanotip fabrication, electrochemical etching of tungsten wire was used in which a 0.3 mm diameter tungsten wire, a graphite tube, and KOH solution in deionized water was applied as anode, cathode, and electrolyte respectively. The most important parameters that govern the nanotip fabrication process are the time delay in turning off the voltage at the end of tip fabrication process, electrolyte concentration, immersion length of the tungsten wire, inner diameter of the cathode tube, and the process voltage. In this research, the effects of these parameters on the radius of nanotip apex were investigated by using Taguchi method. It was found that the process parameters can be ranked in terms of their impact on the radius of nanotip apex as process voltage, electrolyte concentration, wire immersion length, and inner diameter of the cathode tube, respectively. By setting the process parameters on the optimum level, the radius of the nanotip apex was decreased by 5 times in comparison to the mean value of the experimental results. The radius of the nanotip apex was improved down to about 10 nm under the optimum conditions.

Keywords: Nanotip fabrication; Nanotip apex radius; Field Ion Microscope; Scanning Tunneling Microscope

Introduction

Field Ion Microscopy (FIM) and Scanning Tunneling Microscopy (STM) have a wide application in nanoscience and nanotechnology. These microscopes use an ultra sharp metallic tip [1] for imaging the atoms, molecules, and nanostructures. In FIM, decrease of tip-apex radius results in increase of field emitted current

* Corresponding author, Tel.: +98(21)82883368, Fax: +98(21)82883368, E-mail: v_ahmadi@modares.ac.ir

[2], with the consequence of improvement of resolution and magnification of FIM images [3]. STM images resolution is also enhanced by reduction of tip apex radius [4,5,6].

During last decades, a variety of techniques and processes have been developed for fabrication of different metallic tips made from tungsten, platinum, platinum-iridium, gold, and silver [5]. Electrochemical etching process is the most popular method for fabrication of nanotips with desired quality, reliability, and reproducibility [6]. Tungsten is normally the first choice for fabrication of STM tips as it has a high mechanical strength as well as a good electrical conductivity [4,7-12].

For fabrication of STM/FIM nanotips, several researchers [4,7-18] have studied electrochemical etching and some of its related aspects. In researches carried out by Kerfriden et al, it was observed that the length of the lower part of immersed tungsten wire within the range of 10 to 100 mm did not have a significant effect on the characteristics of the apex of the upper part of the wire [4]. To extend the domain of investigations, in the present research, the range of wire immersion length was selected between 2.5 to 7 mm and it was observed that the length of the lower part of the wire less than 7 mm has significant effect on the apex-radius of the nanotip.

For improvement of tip surface smoothness, Xu et al used a constant voltage, with the wire immersed below the nominal air/electrolyte interface by no more than one-half of the wire diameter and stopping the etching at different current levels. This process provided a tip radius range of approximately 100 nm to 5 μm and the surface roughness of about 0.3 nm RMS for a tungsten wire with 0.2 mm diameter [19]. In the present study, tungsten wire diameter of 0.3 mm and wire immersion length of 2.5 to 7 mm was used and the nanotip apex radius of 10 to 80 nm was obtained.

The most important parameters that govern the nanotip fabrication process are the time delay in turning off the voltage at the end of tip fabrication process, the electrolyte concentration, immersion length of the wire, inner diameter of the cathode tube, and the process voltage. Decrease of this time delay and its influence on the tip sharpness have been the subject of researches through design and fabrication of different electronic circuits [8,20-23]. In the present work, an electronic control circuit was designed and implemented for monitoring the process automatically and turning off the voltage within 100 ns. To author's knowledge, optimization of other nanotip fabrication parameters has not been studied so far. In this research, an experimental set-up was designed and constructed for tungsten nanotip fabrication and for gaining minimum radius of the nanotip apex through optimization of the above-mentioned process parameters by using Taguchi method.

Experiments

In the experiments, electrochemical etching of vertically submerged tungsten wire was used for fabrication of the nanotip. Figure 1 shows schematic diagram of the nanotip fabrication process. Pure tungsten wire (99.95 %) with 0.3 mm diameter and a graphite tube was used as anode and cathode, respectively. A DC voltage was applied across these two electrodes. The most common electrolytes used for electrochemical etching of tungsten are KOH and NaOH [17, 20]. In the present research, KOH in deionized water was used as electrolyte. To eliminate the effect of environmental vibrations on the nanotip characteristics, a vibration isolation pad was used under the table.

Experimental Details

The basic electrochemical reactions governing the nanotip fabrication process are as follows [14]:

cathode: $6H_2O + 6e^- \rightarrow 3H_2(g) + 6OH^-$ (1)

anode: $W(s) + 8OH^- \rightarrow WO_4^{2-} + 4H_2O + 6e^-$ (2)

overall: $W(s) + 2OH^- + 2H_2O \rightarrow WO_4^{2-} + 3H_2(g)$ (3)

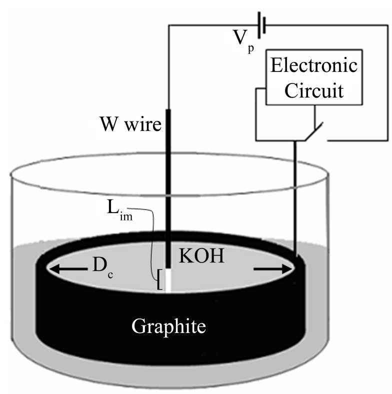

Figure 1. Schematic diagram of nanotip fabrication process; Thickness and height of graphite tube (also, height of electrolyte) are 8 and 20 mm, respectively. Lim, Dc, and Vp are wire immersion length, inner diameter of cathode tube, and process voltage, respectively.

As shown in Fig. 2-a, the electrolyte meniscus is formed around the tungsten wire when the wire is immersed into the electrolyte. The above electro-chemical process generates radial flow of OH^- ions from the cathode graphite tube toward the anode tungsten wire. As shown in Fig. 2-b, the soluble tungstate (WO_4^{2-}) produced during the reaction are directed downwards to the free end of the tungsten wire by the radial flow of OH^- ions and generate a dense viscous layer around the end of wire. According to Fig. 2-b, the etching rate at the bottom of the meniscus is much higher than at the top in region 1. This can be explained by the increase of OH^- density at the bottom of meniscus. Furthermore, the layer of WO_4^{2-} generated around the lower end of wire prevents this region from etching (region 3). Thus, a necking phenomenon occurs at the bottom of the meniscus (region 2). Finally, this part of the wire becomes so thin that its tensile strength cannot sustain the weight of the lower end of the wire (Fig. 2-c); the latter breaks off and a very sharp tip with nanometric apex is left behind (Fig. 2-d). At this moment, if the applied voltage is not turned off, the tip apex starts to be etched and its radius will increase. Therefore, time delay in turning off the voltage has significant impact on the radius of the nanotip apex [9, 23, 24]. In the present work, an electronic circuit was designed and implemented for monitoring the process automatically and turning off the voltage within 100 ns.

Tungsten wire should be perpendicular to the electrolyte surface. Otherwise, fabricated tip will not be in symmetrical form. Fig. 3 shows two samples of fabricated tips with symmetrical and asymmetrical forms.

Design of Experiments Based on the Taguchi Method

To evaluate the effects of process parameters on the radius of nanotip apex, a specially designed experimental procedure is required. Classical experimental design methods are too complex and difficult to use. Additionally, a large number of experiments have to be conducted when the number of process parameters are high. Taguchi method, a powerful tool for reducing the number of experiments, was used to determine optimum process parameters for gaining minimum radius of the nanotip apex. In Taguchi method [25], influencing parameters are separated into two main groups: control factors and noise factors. The control factors are used to select the best conditions for stability in design of fabrication process, whereas the noise factors denote all factors that cause variation. Taguchi proposed to acquire the characteristic data by using orthogonal arrays, and to analyze the performance measure from the data to decide the optimum process parameters. This method uses a special design of orthogonal arrays to study the entire parameter space with small number of experiments only.

According to Taguchi method, the main function of process should be defined at first. In this research, the radius of nanotip apex was defined as the main function of the nanotip fabrication process. The most important influencing process parameters are:

a) **Time delay in turning off the process voltage:** With design and fabrication of an electronic circuit it was fixed at 100 ns.
b) **Electrolyte concentration (E_c):** It was selected between 1 to 4 M/lit.
c) **Tungsten wire immersion length (L_{im}):** In researches curried out by Sophie Kerfriden et al. [4], it was observed that the length of the lower part of tungsten wire within the range of 10 to 100 mm did not have a significant effect on the characteristics of the apex of the upper part of the wire. To extend the domain of investigations, in this research, the range of wire immersion length was selected between 2.5 to 7 mm.

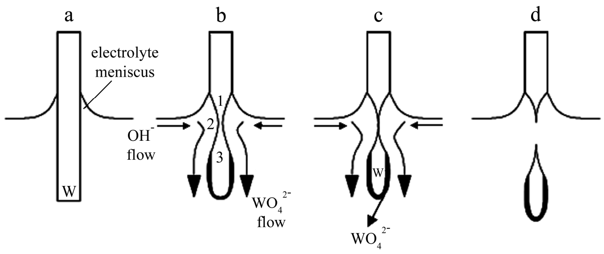

Figure 2. Sequences of nanotip generation.

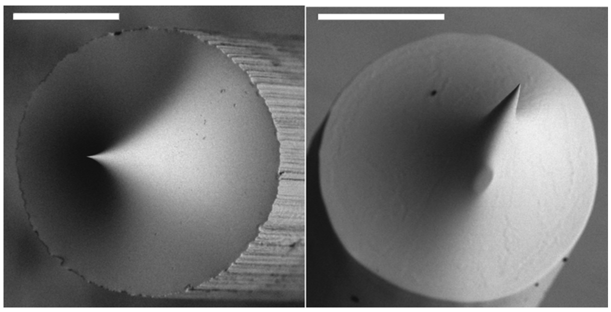

Figure 3. Two fabricated nanotips with symmetrical (left) and asymmetrical (right) forms. In this figures, the white scale bar is equal to 200 μm.

d) **Inner diameter of cathode tube (D_c):** It was selected between 40 to 110 mm.

e) **Process voltage (V_p):** Minimum required voltage for starting anodic dissolution of tungsten in KOH electrolyte, is 1.43 volts [26]. On the other hand, use of a voltage above 4 V causes growth of a thick oxide layer on the tip apex [14]. This prevents the tunneling current in STM. Therefore, the process voltage was selected in the range of 2 to 3.5 volts.

The above-mentioned process parameters were used as control factors and four levels were defined within the given ranges for each parameter as shown in Table 1. To select an appropriate orthogonal array [25, 27] for the experiments, the total degrees of freedom must be computed. The degrees of freedom are defined as the number of comparisons between process parameters that needed to be made to determine which level is better and specifically how much better it is. A four-level process parameter counts for three degrees of freedom. In the present study, the possible interactions between the process parameters are ignored. Therefore, there are 12 degrees of freedom owing to four process parameters in four levels in the nanotip fabrication process.

Once the degrees of freedom are known, the next step is selection of an appropriate orthogonal array to fit the specific task. The degrees of freedom for the orthogonal array should be greater than or at least equal to those for the process parameters. In this study, a L_{16} (4^5) orthogonal array was used because it has 15 degrees of freedom (which is more than the 12 degrees of freedom of the process parameters). This array has five columns and sixteen rows and it can handle five four-level process parameters, at most. Each process parameter is assigned to a column and 16 process parameter combinations are required. Therefore, only 16 experiments are needed to study the entire process parameter space using the L_{16} orthogonal array. The experimental combinations of the process parameters using the L_{16} orthogonal array is presented in Table 2.

The experiments were conducted according to the selected orthogonal array. Then, two series of pictures of the fabricated nanotips were taken by scanning electron microscope (SEM; LEO1455VP) with the magnifications of 100-200X and magnifications of 100-200KX as shown in Figs. 4 and 5, respectively. The experimental conditions used for these results are given in Table 2. The radius of nanotips apex (R_t) was measured by using the latter pictures and the results have been shown in Table 2.

Results

In the Taguchi method [25], a loss function is used to calculate the deviation between the experimental value and the desired value. This loss function is further transformed into a signal-to-noise (S/N) ratio. There are several S/N ratios available depending on type of characteristics; lower is better (LB), nominal is best (NB) and higher is better (HB). In this research, radius of the nanotip apex was selected as the nanotip fabrication process performance characteristic. Lower radius for nanotip apex is the indication of better performance. Therefore, for radius of the nanotip apex "LB" was selected as optimum process performance characteristic. For LB, the S/N ratio (η) for the experimental results can be expressed as:

$$\eta = -10\log_{10}\left(\frac{1}{n}\sum_{i=1}^{n} R_{ti}^2\right) \tag{4}$$

where R_{ti} is the radius of nanotip apex fabricated in ith repeated experiment (nm) and n is the total number of

Table 1. Process parameters and their levels

parameter		Level				Unit
		I	II	III	IV	
E_c	electrolyte concentration	1	2	3	4	M/lit
L_{im}	wire immersion length	2.5	4	5.5	7	mm
D_c	cathode tube inner diameter	40	55	75	110	mm
V_p	process voltage	2	2.5	3	3.5	V

Table 2. Experimental layout using an L_{16} orthogonal array

Expt. No.	E_c	L_{im}	D_c	V_p	R_t nm	signal/noise ratio (dB)
1	1	1	1	1	60	-35.5630
2	1	2	2	2	50	-33.9794
3	1	3	3	3	55	-34.8073
4	1	4	4	4	45	-33.0643
5	2	1	2	4	25	-27.9588
6	2	2	1	3	35	-30.8814
7	2	3	4	2	55	-34.8073
8	2	4	3	1	50	-33.9794
9	3	1	3	2	60	-35.5630
10	3	2	4	1	65	-36.2583
11	3	3	1	4	45	-33.0643
12	3	4	2	3	60	-35.5630
13	4	1	4	3	50	-33.9794
14	4	2	3	4	35	-30.8814
15	4	3	2	1	55	-34.8073
16	4	4	1	2	80	-38.0618

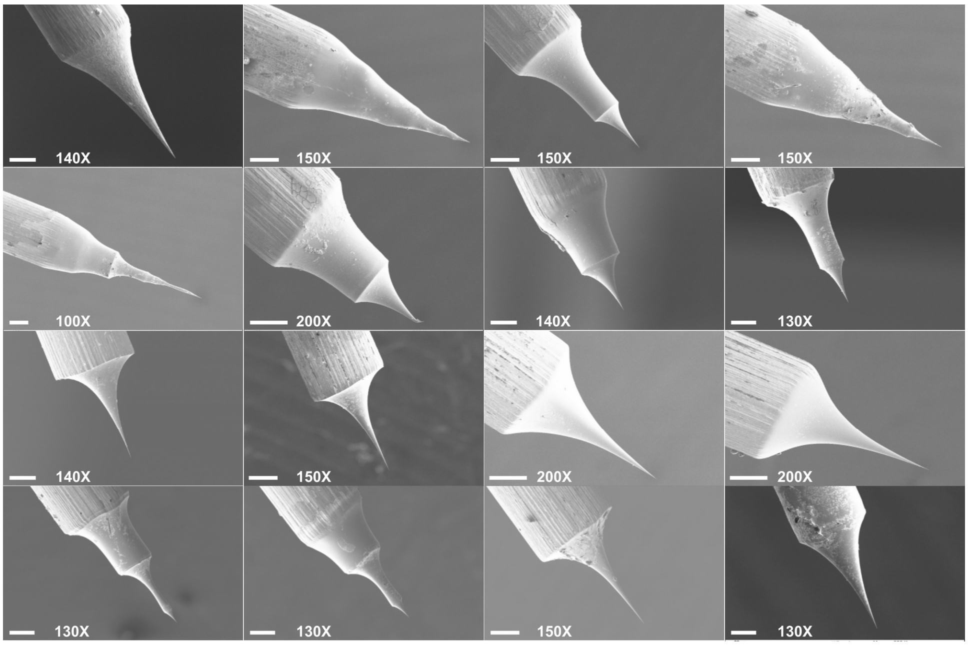

Figure 4. SEM images of the fabricated nanotips taken at magnifications of 100-200X and shown from left to right and up to down corresponding to the experiments No.1-16 of Table 2. In this figures, the white scale bar is equal to 100 μm.

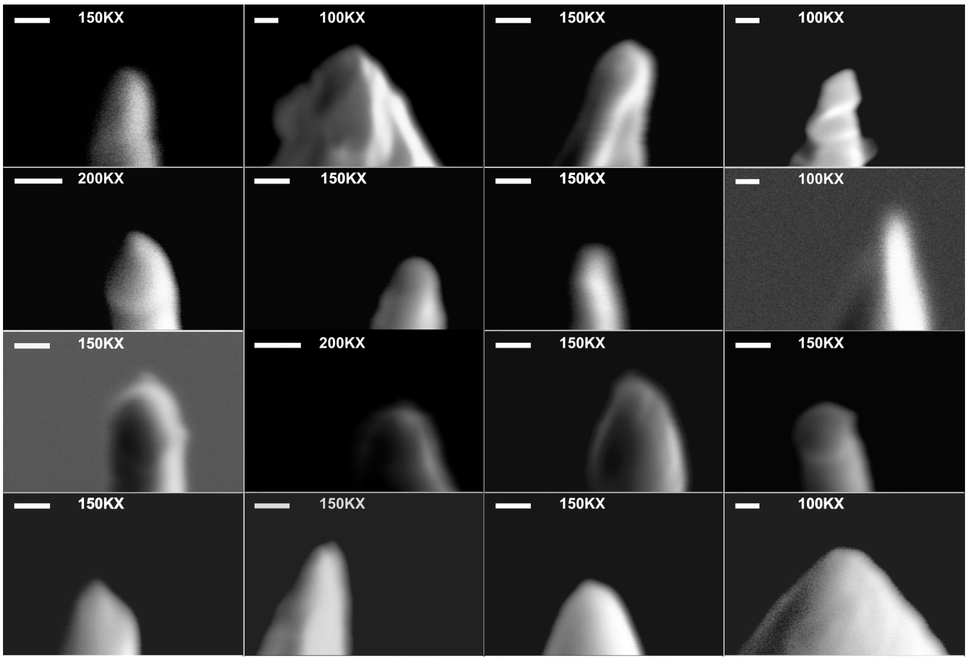

Figure 5. SEM images of apexes of the fabricated nanotips taken at magnifications of 100-200KX and shown from left to right and up to down corresponding to the Expt. No.1-16 of table 2. In this figures, the white scale bar is equal to 100 nm.

repetition of each experiment (n equals 1 in this study). Regardless of category of the performance characteristics, a greater η value corresponds to a better performance. Therefore, the optimum level of the process parameters is the level with the greatest η value. The S/N ratios of L_{16} experiments are shown in Table 2.

The mean values of S/N ratio for the process parameters in different levels are calculated by using the S/N ratio given in Table 2 as below:

$$\bar{\eta}_{ij} = \frac{1}{m}\sum_{k=1}^{m}\eta_{ijk} \tag{5}$$

where $\bar{\eta}_{ij}$ is the mean value of S/N ratio for parameter i in level j, m is the total repetition of level j for parameter i, and η_{ijk} is the S/N ratio related to kth appearance of level j for parameter i. The results of these calculations are shown in Table 3. Influence of different levels of the process parameters on the S/N ratio are shown in Fig. 6. According to the results shown in Table 3 and Fig. 6, it can be concluded that:

1. **Electrolyte concentration (E_c):** Curve of E_c shows a maximum for S/N ratio at 2 M/lit. This corresponds to minimum value for the radius of nanotip apex.
2. **Tungsten wire immersion length (L_{im}):** The radius of nanotip apex has a little decrease with wire immersion length up to 4 mm but beyond that it increases.
3. **Inner diameter of cathode tube (D_c):** with increase of inner diameter of the cathode tube to 55 mm, the radius of the nanotip apex decreases and more than 55 mm, the radius increases.
4. **Process voltage (V_p):** With ignoring a little reduction of the S/N ratio from 2 to 2.5 V, the radius of nanotip apex decreases inversely with process voltage up to 3.5 V. It must be regarded that at more voltages a thick oxide layer appears on the apex of the tip.

Therefore, optimum level of the process parameters for minimum radius of the nanotip apex are electrolyte concentration of 2 M/lit (level 2), wire immersion length of 4 mm (level 2), cathode tube inner diameter of 55 mm (level 2), and process voltage of 3.5 V (level 4).

The relative effect of different process parameters on the radius of nanotip apex was obtained by analysis of variance (ANOVA). The relative importance of influence of the process parameters on the radius of nanotip apex was investigated to determine more accurately the optimum combinations of the process parameters by using ANOVA [25, 27]. In this analysis method, total sum of dispersion squares (S_{total}) is calculated by

$$S_{total} = \sum_{i=1}^{p}\left(\eta_i - \eta_m\right)^2, \tag{6}$$

where p is the total number of experiments, η_i is the S/N ratio of the ith experiment, and η_m is the overall mean of S/N ratio.

For each parameter, sum of squares (the difference between the average sum of the square of total S/N ratios at each level and the ratio of square of the total sum of S/N ratios divided by total number of experiments) (S_{E_c} for parameter E_c) is given by

$$S_{E_c} = \frac{1}{N_{E_c}}\left[E_c(1)^2 + E_c(2)^2 + E_c(3)^2 + E_c(4)^2\right] - \frac{T^2}{N}, \tag{7}$$

where $E_c(1)$, $E_c(2)$, $E_c(3)$, and $E_c(4)$ are the sum of S/N ratio of experiments with parameter E_c at levels 1, 2, 3 and 4, respectively and N_{E_c} is the repetition of each level of parameter E_c. T is the sum of total S/N ratio of the experiments and N is the total number of experiments. A similar $S_{L_{im}}$, S_{D_c} and S_{V_p} values were calculated for L_{im}, D_c and V_p.

The error sum of squares (S_e) is calculated as below:

$$S_e = S_{total} - \left(S_{E_c} + S_{L_{im}} + S_{D_c} + S_{V_p}\right) \tag{8}$$

Table 3. The mean value of S/N ratio for process parameters in different levels

Level	S/N (dB)			
	E_c	L_{im}	D_c	V_p
I	-34.35	-33.27	-34.39	-35.15
II	**-31.91**	**-33.00**	**-33.08**	-35.60
III	-35.11	-34.37	-33.81	-33.81
IV	-34.43	-35.17	-34.53	**-31.24**

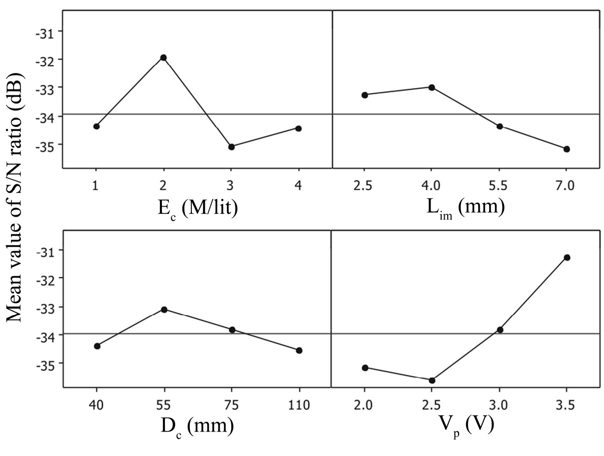

Figure 6. Mean value of S/N ratios of nanotip apex radius against different levels of process parameters.

Table 4. Analysis of variance of the S/N ratio for process parameters

Source	Degree of freedom (f)		Sum of Squares (S)	Variance (V) = (S/f)	F-ratio = (V/V_e)	[3]P(%) = (S/S_{total}) * 100
E_c	[1]L -1 =	3	23.685	7.8949	17.16	26.7
L_{im}		3	12.116	4.0388	8.78	13.7
D_c		3	5.245	1.7484	3.80	5.9
V_p		3	46.117	15.3725	33.40	52.1
Error (e)	15-(4*3) =	3	1.381	0.4602		1.6
Total	[2]N-1 =	15	88.544			100

[1]L: number of level for each parameter
[2]N: total number of experiments
[3]P: percentage contribution

Calculation of other factors of ANOVA; degree of freedom, variance, F-ratio, and percentage contribution are described in Table 4.

The results of ANOVA for the process parameters are presented in Table 4. The greater values of F-ratio and percentage contribution for a parameter determine the more impact on the radius of nanotip apex. Therefore, the process parameters can be ranked in terms of their impact on the radius of nanotip apex as process voltage, electrolyte concentration, wire immersion length, and inner diameter of the cathode tube, respectively.

Discussion

According to Figure 2(b-d), it is observed that the necked region becomes thinner and more lengthened by effect of etching and elongation under load w_L (weight of the lower part of the wire) until the lower part of the wire is separated. The sequences of nanotip fabrication can be divided into three stages; 1) before separation of the lower part of the wire 2) moment of separation 3) after separation.

The sum of effects of these three stages determines the final apex-radius of the nanotip. The drastically influencing factors on the nanotip apex radius in mentioned stages can be summarized as follow:

1. The amount of d_w (minimum diameter of the tungsten wire at the necked region) at the end of the first stage; smaller d_w results in smaller apex-radius.
2. At the second stage, the mechanism of separation of the last atoms at the necked region is under influence of etching performance. Chemical composition and ion orientation within the adjacent layers to the neck and physical behavior of the layers like motions within the layers and beyond them, electrical attraction or repulsion of the ions to the necked material and potential gradient nearby the neck determine the etching performance. Meanwhile, fine separation of the lower part of the wire is affected by proper combination of etching of the necked region and its simultaneous stretching under w_L.
3. At the third stage, during time delay in turning off the voltage, the nanotip apex starts to be etched and its radius will increase. Therefore, the etching rate can affect the nanotip apex radius at this stage; the higher the etching rate the higher the apex-radius.

The d_w is a function of etching rate and elongation rate of the necked region. The w_L is a function of L_{im}, etching rate of the lower part of the wire, and the amount of the tungstate deposited on the lower part of the wire during the process.

The above-mentioned stages are functions of interaction of etching rate and elongation rate which themselves are dependent upon the E_c, L_{im}, D_c and V_p.

It seems that, if the etching rate is low, the selective etching from the neck diminishes and the whole body immersed into the electrolyte will be attacked almost uniformly. Therefore, w_L and d_w will decrease almost with the same rate. Consequently, the elongation of the necked region and reduction of d_w will be low at the first stage and the final apex-radius will be high. On the other hand, if the etching rate is high the opportunity of elongation of the necked region during the first stage will be low and during the second stage the dominant mechanism of separation will be etching. Consequently, again, the nanotip apex radius will be high. If the etching rate of the necked region is in proper interaction with its elongation rate (optimum etching rate), reduction of d_w and elongation of necked region will be high during the first stage. This will provide the necked region to be lengthened further at later stages of etching, leading to separation of the lower part of the wire. This will give rise to low nanotip apex radius.

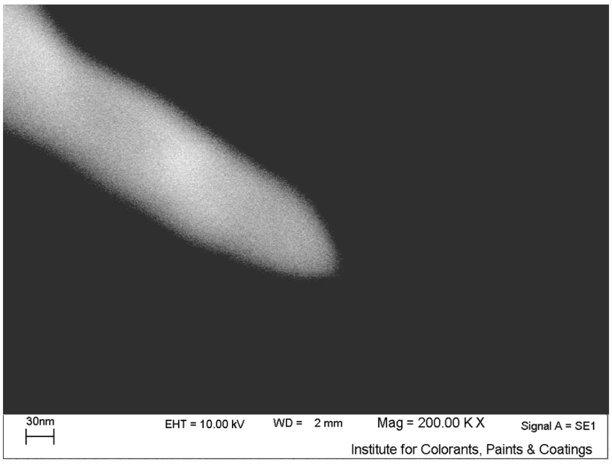

Figure 7. Image of the nanotip apex with minimized radius.

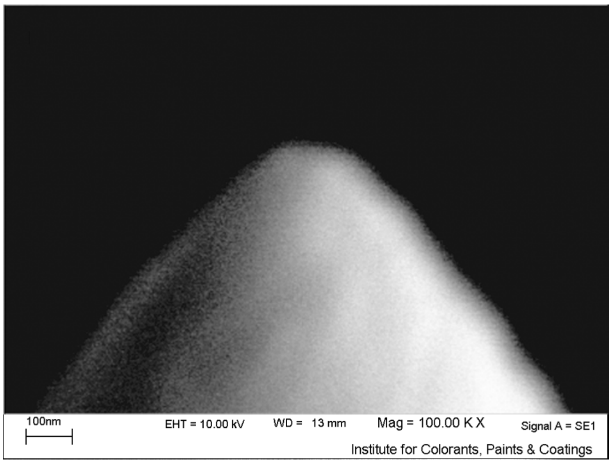

Figure 8. Image of apex of fabricated nanotip in experiment No. 16.

Confirmation Test

The confirmation test was the final step in optimization of nanotip apex radius based on the Taguchi method results. After determining the optimum levels of nanotip fabrication parameters, a new experiment was conducted by setting the parameters on the optimum level. In this experiment, the achieved nanotip apex radius was about 10 nm and the S/N ratio was -20 dB. The improvement of S/N ratio was 13.9512 dB and the radius of nanotip apex was decreased by 5 times in comparison to the mean value of experimental results shown in Table 2. SEM image of the apex of the fabricated nanotip with minimized radius is shown in Fig. 7 and, for comparison, the SEM image of apex of fabricated nanotip in experiment No. 16 is shown in Figure 8.

In this paper, influence of the parameters of nanotip fabrication process on the radius of nanotip apex was investigated by using Taguchi method. The combination of optimum level of process parameters was obtained by using the analysis of signal-to-noise (S/N) ratio. The level of importance of effect of the process parameters on the nanotip apex radius was determined by using the analysis of variance (ANOVA). It was found that the optimum level of the process parameters for gaining minimum radius of the nanotip apex is electrolyte concentration of 2 M/lit, wire immersion length of 4 mm, cathode tube inner diameter of 55 mm, and voltage of 3.5 V within the range of experiments. The process parameters can be ranked in terms of their impact on the radius of nanotip apex as process voltage, electrolyte concentration, wire immersion length, and inner diameter of the cathode tube, respectively. By setting the process parameters on the optimum level, the radius of nanotip apex was decreased 5 times in comparison to the mean value of the experimental results. The minimum nanotip apex radius of about 10 nm was achieved under the optimum conditions.

References

1. Melmed A.J. The Art and Science and Other Aspects of Making Sharp Tips. *J. Vac. Sci. Technol.,* B **9**: 601-608 (1991).
2. Gomer R. *Field Emission and Field Ionization.* Harvard University Press (1961).
3. Miller M.K., Cerezo A., Hetherington M.G., and Smith G.D. *Atom Probe Field Ion Microscopy.* Oxford University Press (1996).
4. Kerfriden S., Nahle A.H., Campbellm S.A., Walsh F.C. and Smiths J.R. The electrochemical etching of tungsten STM tips. *Electrochimica Acta,* **43**: 1939-1944 (1998).
5. Boyle M.G., Feng L. and Dawson P. Safe fabrication of sharp gold tips for light emission in scanning tunneling microscopy. *Ultramicroscopy,* **108**: 558-566 (2008).
6. Kazinczi R., Szocs E., Kalman E. and Nagy P. Novel Methods for Preparing STM tips. *Appl. Phys.,* A **66**: 535-538 (1998).
7. Muller A.D., Muller F., Hietschold M., Demming F., Jersch J. and Dickman K. Characterization of electrochemically etched tungsten tips for scanning tunneling microscopy. *Rev. Sci. Instrum.,* **70**: 3970-3972 (1999).
8. Schmidt U., Rasch H., Fries Th., Röllgen F.W. and Wandelt K. Characterization of STM W-tips by FIM with an organic image gas. *Surface Science,* **266**: 249-252 (1992).
9. Méndez J., Luna M. and Baro A.M. Preparation of STM W tips and characterization by FEM, TEM and SEM. *Surface Science,* **266**: 294-298 (1992).
10. Hockett L.A. and Creager S.E. A convenient method for removing surface oxides from tungsten STM tips. *Rev. Sci. Instrum.,* **64**: 263-264 (1993).

11. Oliva A.I., Romero A.G., Pena J.L., Anguiano E. and Aguilar M. Electrochemical preparation of tungsten tips for a scanning tunneling microscope. *Rev. Sci. Instrum.,* **67**: 1917-1921 (1996).
12. Ottaviano L., Lozzi L. and Santucci S. Scanning Auger microscopy study of W tips for scanning tunneling microscopy. *Rev. Sci. Instrum.,* **74**: 3368-3378 (2003).
13. Lemke H., Goddenhenrich T., Bochem H.P., Hartmann U. and Heiden C. Improved microtips for scanning probe microscopy. *Rev. Sci. Instrum.,* **61**: 2538-2541 (1990).
14. Ibe J.P., Bey P.P., Brandow S.L., Brizzolara R.A., Burnham N.A., DiLella D.P., Lee K.P., Marrian C.R.K. and Colton R.J. On the Electrochemical Etching of Tips for Scanning Tunneling Microscopy. *J. Vac. Sci. Technol.,* A **8**: 3570-3575 (1990).
15. Fainchtein R. and Zarriello P.R. A computer-controlled technique for electrochemical STM tip fabrication. *Ultramicroscopy,* **42**: 1533-1537 (1992).
16. Bourque H. and Leblanc R.M. Electrochemical fabrication of scanning tunneling microscopy tips without an electronic shut-off control. *Rev. Sci. Instrum.,* **66**: 2695-2697 (1995).
17. Klein M. and Schwitzgebel G. An improved lamellae drop-off technique for sharp tip preparation in scanning tunneling microscopy. *Rev. Sci. Instrum.,* **68**: 3099-3103 (1997).
18. Kar A.K., Gangopadhyay S., Mathur B.K. and Gangopadhyaym S. A reverse electrochemical floating-layer technique of SPM tip preparation. *Meas. Sci. Technol.,* **11**: 1426-1431 (2000).
19. Xu D., Liechti K.M. and Ravi-Chandar K. Mesoscale scanning probe tips with subnanometer rms roughness. *Rev. Sci. Instrum.,* Doi:10.1063/1.2756997 (2007).
20. Krakauer B.W., Hu J.G., Kuo S.M., Mallick R.L., Seki A., Seidman D.N., Baker J.P. and Loyd R. A system for systematically preparing atom-probe field-ion-microscope specimens for the study of internal interfaces. *Rev. Sci. Instrum.,* **61**: 3390-3398 (1990).
21. Krakauer B.W. and Seidman D. N. Systematic procedures for atom-probe field-ion microscopy studies of grain boundary segregation. *Rev. Sci. Instrum.,* **63**: 4071-4079 (1992).
22. Morgan R. An automatic electropolishing supervisor for preparing field ion microscope specimens. *J. Sci. Instrum.,* **44**: 808-809 (1967).
23. Chen Y., Xu W. and Huang J. A single new technique for preparing STM tips. *J. Phys. E: Sci. Instrum.,* **22**: 455-457 (1989).
24. Tsong T.T. *Atom-Probe Field Ion Microscopy.* Cambridge: Cambridge University Press (1990).
25. Ross P.J. *Taguchi Techniques for Quality Engineering.* New York: McGraw-Hill (1989).
26. Evans U.R. *The Corrosion and Oxidation of Metals.* London: Arnold (1960).
27. Phadke M.S. *Quality Engineering Using Robust Design.* New Jersey: Prentice Hall (1989).